proceedings of THE 17th NEW ZEALAND GEOTHERMAL WORKSHOP 1995

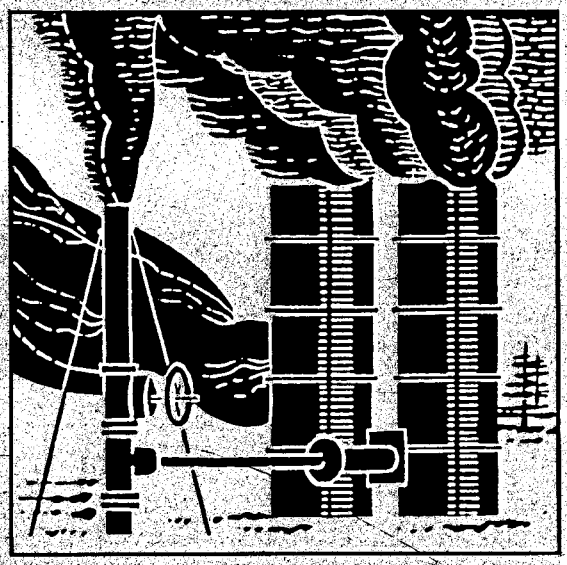

compiled and edited by
M. P. Hochstein, J. Brotheridge and S.F. Simmons

presented by
Geothermal Institute
The University of Auckland
in conjunction with
The Centre for Continuing Education

DISCLAIMER

INVERSE MODELLING OF THE KAWERAU GEOTHERMAL RESERVOIR, NZ

S.P. WHITE

NZ Institute for Industrial Research and Development, Lower Hutt, NZ

SUMMARY – In this paper we describe an existing model of the Kawerau geothermal field and attempts to improve this model using inverse modelling techniques. A match of model results to natural state temperatures and pressures at three reference depths are presented. These are used to form and 'objective function' to be minimised by inverse modelling.

1 Introduction

In this paper we will describe an existing model of the Kawerau geothermal field which represents about the best fit we could obtain to measured pressures and temperatures using the traditional ("suck it and see") method of adjusting parameters. Then we will compare these results with results obtained using an inverse modelling technique recently developed by Finsterle and Pruess (1995).

The first large scale numerical model of the Kawerau geothermal field was completed in 1987 and is described in McGuinness & White (1991). This gave a good match to the measured decline in production enthalpy prior to 1987. The match to more recent production data is less satisfactory. For all the main production wells (KA19, KA35, KA21), predicted temperature rundowns exceed measured values.

The 1987 model used the results of a resistivity survey described in MacDonald et al (1970) carried out in 1969-70. Areas of the model outside the area of low resistivity defined by this survey were taken to be cold. Resistivities obtained by this survey were representative of values to a depth of about 250 metres. For want of any better information it was assumed these values also applied to much greater depths. In 1989 a second resistivity survey was carried out, Dawson et al (1989), with the aim of obtaining resistivity measurements at greater depths (about 500 metres). A key feature of the deeper survey is a major extension of the low resistivity area to the east of the mill (see Figure 1). The significance of this low resistivity area to the east is not yet clear. It may indicate a large extension to the hot reservoir or perhaps be the result of much earlier activity and therefore not represent a significant increase in the potential of the reservoir. In the modelling described here it is treated as a "warm" area of moderate permeability below a depth of 500 metres.

Recent drilling at Kawerau has concentrated on intersecting the faults that cut the field. This approach has been very successful. KA19 and KA21 have both been good long-term production wells with very little temperature rundown. By producing from faults, these wells are isolated to some extent from the major cooling mechanism thought to operate at Kawerau, the drawing-in of cool water from shallow levels or from outside the boundaries of the field. Incorporating the effects of faults in the field on production wells is an important feature of the model described here.

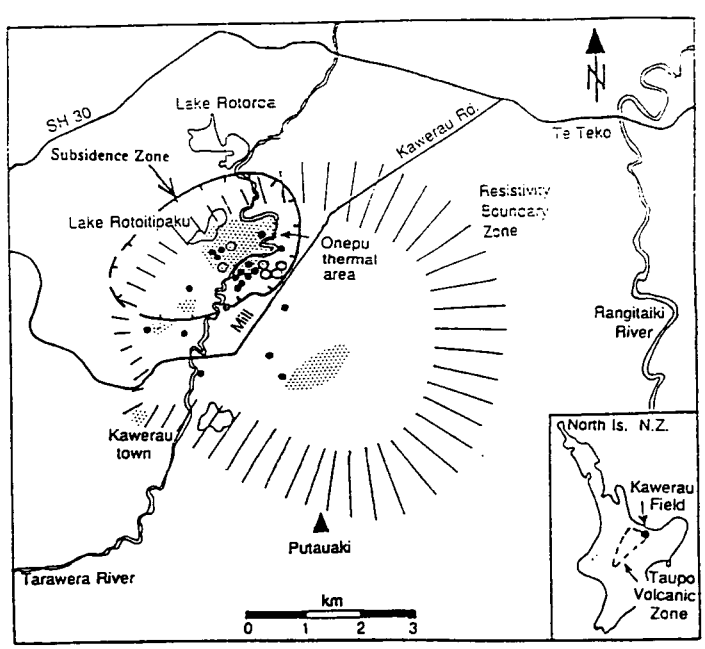

Figure 1: Kawerau Reservoir Area

1.1 Modelling of Faults

When faults are included they are modelled as narrow areas (a few metres) of enhanced permeability. It has been necessary

to make all faults vertical in order to simplify modelling. Including faults gives a much better match to the natural state of the field (average error = 3% for model with faults; = 4% for model without faults). Also the maximum error without faults was 30% compared to 17% when faults are included.

2 Model Description

The numerical model described in this report is based on the conceptual model described by Allis *et al.*(1993).

The MULKOM (Pruess 1982) model developed here covers an area 10 km 10 km encompassing the most recent resistivity boundary and extending as far south as Mt Edgecumbe. Vertically the model extends from deep in the greywacke basement, at a depth of 3.5 km, up to the surface.

The model is divided into 15 horizontal layers of varying thickness as shown in Figure 2. Each layer is divided into a number of blocks. The spatial resolution of the model is controlled by the size of blocks in a layer and the thickness of the layer. Blocks are smallest (and thus resolution is greatest) in areas of current and future production. Calculated temperatures, pressures and saturations represent average values for a block. In the production area of the field, blocks are about 250 metres square. Where accuracy is less important 2 km square blocks are used. A typical layer from the production area of the field is shown in Figure 3.

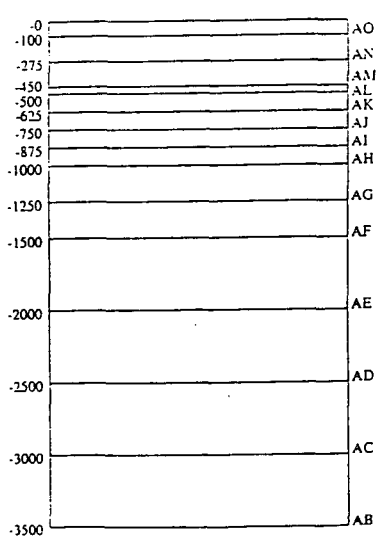

Figure 2: Vertical Subdivisions

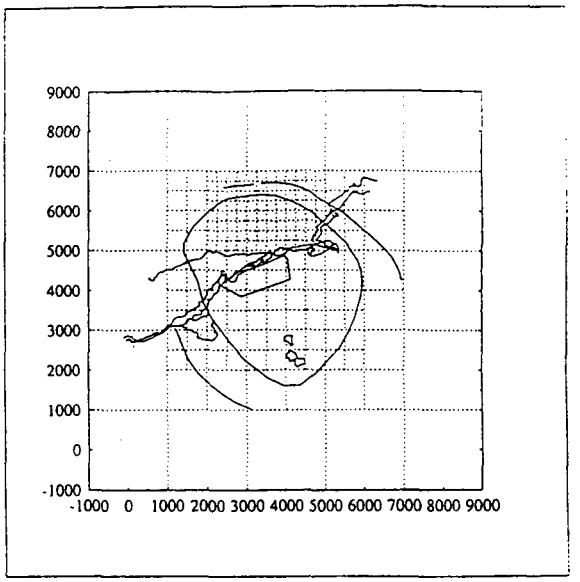

Figure 3: Horizontal Subdivisions

The geology of the drilled area of the field is very complex. Basement greywacke is overlain by about 13 different units, including rhyolites, breccias, andesites, tuffs, sediments and ignimbrites. Currently production is from fractured greywacke or andesite. It is believed the Huka sediments and ignimbrite act as aquacludes over areas of the field. Where possible, geological data from Allis *et al.* (1993) were used to assign a rock type to each element. Where no geological information is available, rock types assigned to an element represent a best guess of the correct type.

The geology at Kawerau had led MacDonald *et al.* (1970) to associate permeability with fracturing. These authors and Nairn (1982) note that the best production at Kawerau originates either in the basement greywacke or the andesite. Both of these rocks have low intrinsic permeability. The importance of faults to production has already been mentioned but interference tests show permeability is not limited to the major faults (or else that major faults may be more widespread than currently mapped).

These factors led to a model of the field with a deep hot source in the vicinity of Mt Edgecumbe, with the hot source fluid moving predominantly through faults and permeable zones in the basement greywacke, and mixing with cooler waters flowing horizontally across the field. Secondary permeability is provided by fracturing of brittle rock types and this provides a pathway for interaction between the geothermal fluids and larger volumes of rock than is accessed by the known faults in the system.

Known faults have been included in the model and are represented as areas of enhanced permeability. It is assumed that rocks outside the resistivity boundary have not been subjected to the same thermal stresses as those within the boundary, and consequently permeabilities will not have been enhanced by hydrothermal fracturing.

2.1 Boundary Conditions

It is believed that the model covers a large enough area for boundary temperatures to be given by the normal geophysical temperature gradient (assumed to be 30° C/km), and for pressures to be hydrostatic. There is a regional flow from the south-east to the northwest and this is incorporated into the boundary conditions by fixing pressures to be hydrostatic on the boundaries at y = 0 km and y = 10 km.

Temperature at the surface is taken to be 20° C and increases with depth (see above). The surface of the model is 125 metres higher at the y = 0 boundary than at the y = 10 km boundary. The difference in height of the groundwater levels on the two boundaries is 260 metres which results in a pressure gradient of about 2.5 bars/kilometre in the y direction (roughly SE-NW) of the model.

No flow is permitted across the bottom of the model or across the boundaries at x = 0 and x = 10 km.

At the surface of the model is air at 20° C and one bar. It is possible for water to flow out of the surface of the model and for air to flow into the model. This allows the groundwater level to be below the surface of the model with a vadose zone between the groundwater level and the surface of the model. To simulate rainfall, water with an enthalpy of 840 kJ/kg (20° C) is injected into the top layer of elements at a rate of 2.9 kg/s/km^2.

Most of the heat flow to the surface at Kawerau is into the river and this is simulated by a series of pressure dependent fluid sinks along the path of the river. A deep source under the southern part of the field produces an inflow of approximately 200 MW of heat and 100 kg/s fluid.

3 The Natural State

3.1 Manual Method

As a first step in assigning rock properties, a rock type (eg, andesite, greywacke, etc) was assigned to each model element. Values for permeability, porosity and density were assigned to each rock type. These values were obtained from previous estimates of reservoir properties from interference tests and the like. Where no information was available the values chosen were simply guesses.

Grant [Mongillo, Chapter 14] has analysed all the early pressure and temperature measurements from Kawerau and adjusted the data to one of three reference levels at 750 metres, 1050 metres, and 1400 metres below sea level. This data of Grant, together with data not available to Grant, was used to adjust the permeabilities.

The procedure followed was to run the model until a steady state was reached then a 'goodness of fit' to measurement was calculated. This goodness of fit (SS) is defined by

$$SS = \sum_{i=1}^{N_{\text{meas}}} \frac{|X_i - X_{\text{meas}}|}{X_{\text{meas}}} \qquad (1)$$

where X_i is the calculated value of pressure of temperature and X_{meas} is the measured value. SS is the average relative error in the calculated values ($N_{\text{meas}} = 55$ is the number of measured data points).

Permeabilities and inflows were adjusted to approximately minimise SS. The final value achieved for the model containing fractures was SS = .03 which represents an average error in calculated values of 3%. It must be remembered that data are only available over a small part of the modelled volume.

3.2 Natural State Flows

The three flows into the field which define the natural state are:

1. A hot upflow originating at great depth. In the model the hot fluid is injected into an element connected to layer AB over the area and (x and y refer to the model coordinate system). Inflow rate is 70 kg/s and the enthalpy of the injected fluid is 2000 kJ/kg. This results in temperatures of up to 360° C at the bottom of the model.

2. A regional cross-flow of cooler fluid. In the model the flow is from y = 0 towards y = 8000. This corresponds to a flow from the south east to the north west. The hydrostatic head on the y = 0 boundary is higher than that on the y = 8000 boundary and thus the cooler fluid is driven into the reservoir at y = 0, mixes with the hot upflow and exits towards the y = 8000 boundary or through the surface.

3. A flow of hot fluid into the sinks along the river and a loss of heat by conduction. The estimated flow of heat to the river is 70 MW (Allis et al Chapter 1) and this compares with 60 MW calculated by the model. Mass flow to the river is approximately 87 kg/s.

Figure 4 is a cartoon showing the important flows in the field.

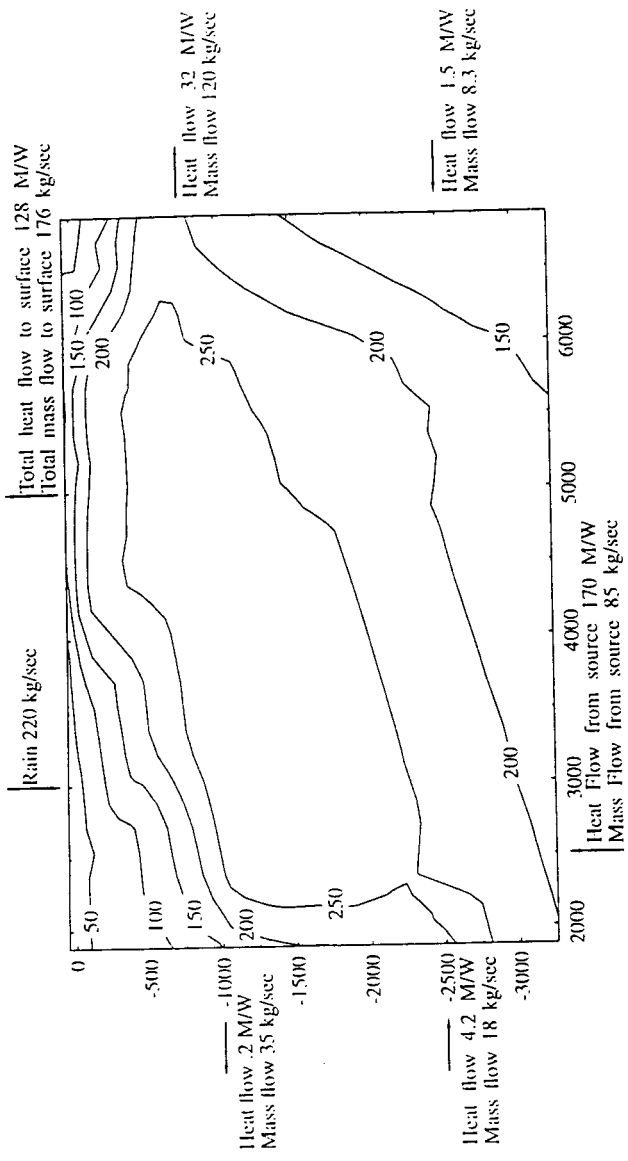

Figure 4: Temperature contours on a cross section at x = 5000 meters, also shown are boundary flows. All distances are in meters and temperature contours are labelled in ° C.

3.3 Match to measured data

In Figure 5 we plot the relative error in pressure value. Apart from one outlier (KA26) with a 12% error in pressure at 750 metres, almost all the other errors are less than 3% and are distributed more or less evenly about zero. KA26 lies in the south west of the field, well separated from most of the other wells (apart from KA29) and has very poor permeability. There is also an outlier in the calculated temperatures at the nearby KA29.

Figure 6 is a similar plot of errors in calculated temperatures. In this case the errors are also reasonably evenly distributed about zero and in most cases are within +/- 5%. There is an obvious outlier at 1050 metres with an error of 17%. This is in well KA29 which is located in the south west of the field 80 metres north of KA26 (the location of the largest error in pressure).

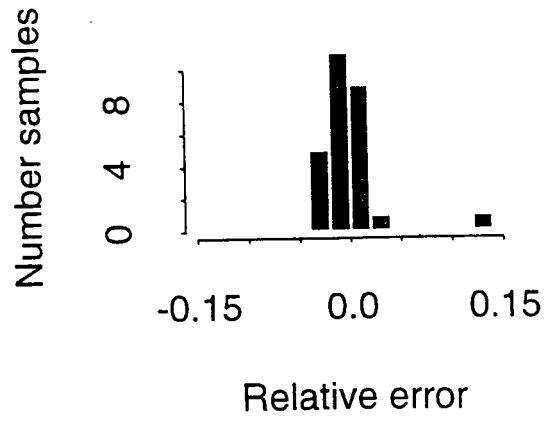

Figure 5: Relative errors in pressure (manual method)

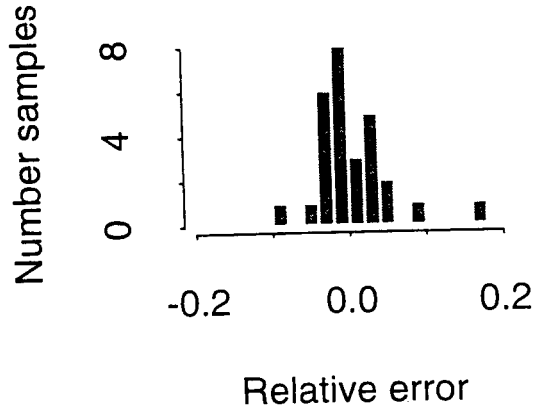

Figure 6: Relative errors in temperature (manual method)

3.4 Inverse Modelling

ITOUGH2 formalises the intuitive approach described in section 3.1 by minimising an objective function calculated from the differences between the model solution and measured data. There are several functional forms of the objective function available, the advantages of the different forms are discussed in Finsterle (1993). For the work described here we have used the default objective function which is a **quadratic** function of the residuals . Note that for the manual method we used a **linear** objective function. The effect of the quadratic objective function is to emphasize the importance of outliers on the objective function. In hind site, it would have been better to choose a linear objective function or one based on a robust estimator as

this would have made the comparision with the manual method easier.

The approach taken was to take the model used in the manual method and allow ITOUGH2 to vary ten permeabilities in order to reduce the objective function. We used an option that initially calculated the sensitivities of all the parameters and only those with large sensitivities were varied in an attempt to reduce the objective function. All the sensitivities were recalculated each 3 iterations. This reduced the original ten parameters to about five for most of the calculation. After 16 iterations (requiring about 140 TOUGH2 runs) the objective function was reduced to 61% of its original value. While this point was not regarded as a minimum by ITOUGH2 the results presented in this paper are taken from there. The original parameters and the new values of the parameters are presented in Table 1.

Rock type	Original	Final	Sensitivity
ROK07xy	5.00e-16	5.00e-16	.1
ROK07z	7.08e-16	6.45e-16	10.3
ROK08xy	1.00e-12	1.00e-12	.1
ROK08z	1.37e-12	1.17e-12	.4
ROK09xy	1.68e-17	1.00e-18	.7
ROK09z	1.39e-15	6.88e-16	7.4
ROK05xy	2.00e-15	2.00e-15	.1
ROK05z	2.00e-15	2.00e-15	.1
ROK11xy	3.89e-14	2.78e-14	.5
ROK11z	2.00e-14	2.00e-14	.1
ROK06xy	1.19e-13	9.78e-14	.3
ROK06z	8.00e-14	8.00e-14	.3
ROK03xy	3.49e-14	1.24e-14	6.5
ROK03z	4.29e-13	1.75e-14	.6

Table 1: Rock Permeabilities (units are m^2)

The sensitivities presented in Table1 are a measure of the dependence of the importance of the parameters on the value of the objective function. A large sensitivity indicates that small changes in a parameter causes large changes in the objective function. We see from Table 1 that the most important parameter is ROK07z which is the vertical permeability of the huka formation which provides a partial cap to the field at around 500 meters depth. The other important parameters are the vertical permeability of the Opnoke ignimbrite (ROK09) which provides a flow barrier in the southern part of the field and the horizontal permeability in the basement greywacke (ROK03).

Also provided are estimates of the standard deviation for the distributions of the estimated parameters which provide a range within which we expect the parameter to lie. For the three most important parameters the estimated range ($\pm 3\sigma$) is given in Table 2.

Parameter	Minimum	Mean	Maximum
ROK07z	4.20×10^{-16}	6.45×10^{-16}	9.80×10^{-16}
ROK09z	3.80×10^{-16}	6.88×10^{-16}	1.26×10^{-15}
ROK03xy	1.12×10^{-14}	1.24×10^{-14}	2.82×10^{-14}

Table 2: Range estimates for important parameters.

Unfortunately the very large amounts of computer time required for a ITOUGH2 run precluded any experimentation with different optimisation functions. We have also added a number of extra data points for the ITOUGH2 run. These were added in an attempt to improve the vertical temperature distribution in the south of the field. Unfortunately this means a direct comparision between figures 5 and 7 or 6 and 8 cannot be made.

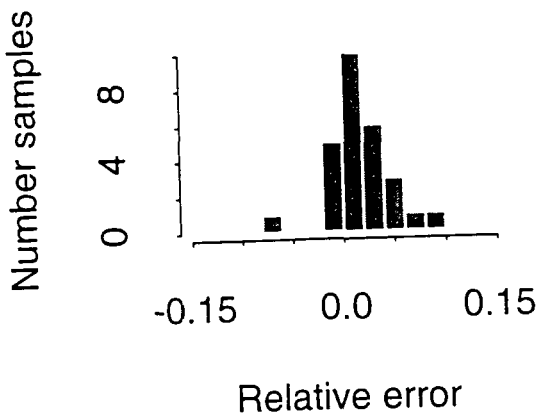

Figure 7: Relative errors in pressure (ITOUGH2)

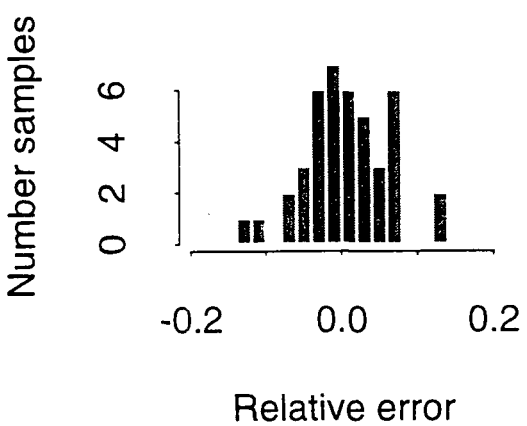

Figure 8: Relative errors in temperature (ITOUGH2)

4 Conclusions

A good match to what data were available on the natural state pressures and temperatures has been obtained both with conventional modelling and with ITOUGH2. Unfortunately we cannot directly compare the "goodness of fit" of the two models as the number of data points was increased for the ITOUGH2 run and a quadratic objective function was used. The quadratic objective function has the effect of reducing the largest error but the cost is an increase in the average error.

The real benefit of using ITOUGH2 in this work was the excellent error analysis that is provided. The manual method provides no reliable way to estimate how good parameter estimates are. ITOUGH2 provides estimates of the standard deviations of the estimated parameters which are essential for investigating "worst-case" scenarios when the field is produced.

5 References

Allis, R.G., Christenson, B.W., Nairn, I.A., Risk, G.F. and White, S.P. (1993). The natural state of the Kawerau geothermal field. Proc. 15th N.Z. Geothermal Workshop.

Dawson G B, Bibby H M, Bennie S L, Rayner H H, Risk G F (1989). "Electrical Resistivity Survey of the Kawerau Geothermal Field and the Surrounding Region", Contract Report No 126 for GGT, Geophysics Division DSIR.

Finsterle S., "ITOUGH2 User's Guide Version 2.2". Report LBL-34581, Lawrence Berkeley Laboratory.

MacDonald WJP, Muffler LJP, Dawson G B (1970). "Geophysical Investigations at Kawerau", Geophysics Division Report No 4, DSIR Wellington.

McGuinness, M.J., White, S.P. (1991). Modelling of the Kawerau geothermal field. Proc. 13th N.Z. Geothermal Workshop.

Mongillo M A (ed) (1986). "Kawerau Geothermal Field DSIR Geothermal Report Number 10".

Nairn I A (1982). "Geology of Kawerau Geothermal Field (MKII), Results of Drilling, 1977-1982", Geothermal Circular IAN4, NZGS, DSIR Rotorua.

Pruess K (1982). "Development of the General Purpose Simulator MULKOM", Report LBL-15500, Lawrence Berkeley Laboratory.

White S P, McGuinness M J (1990). "Kawerau Modelling Scenarios II", DSIR Applied Mathematics Report 161.